NASA/TM–2010-216201

# Evaluation of a Small-Crack Monitoring System

*John A. Newman*
*Langley Research Center, Hampton, Virginia*

*William M. Johnston*
*Lockheed Martin Mission Services*
*Langley Research Center, Hampton, Virginia*

February 2010

## NASA STI Program . . . in Profile

Since its founding, NASA has been dedicated to the advancement of aeronautics and space science. The NASA scientific and technical information (STI) program plays a key part in helping NASA maintain this important role.

The NASA STI program operates under the auspices of the Agency Chief Information Officer. It collects, organizes, provides for archiving, and disseminates NASA's STI. The NASA STI program provides access to the NASA Aeronautics and Space Database and its public interface, the NASA Technical Report Server, thus providing one of the largest collections of aeronautical and space science STI in the world. Results are published in both non-NASA channels and by NASA in the NASA STI Report Series, which includes the following report types:

- TECHNICAL PUBLICATION. Reports of completed research or a major significant phase of research that present the results of NASA programs and include extensive data or theoretical analysis. Includes compilations of significant scientific and technical data and information deemed to be of continuing reference value. NASA counterpart of peer-reviewed formal professional papers, but having less stringent limitations on manuscript length and extent of graphic presentations.

- TECHNICAL MEMORANDUM. Scientific and technical findings that are preliminary or of specialized interest, e.g., quick release reports, working papers, and bibliographies that contain minimal annotation. Does not contain extensive analysis.

- CONTRACTOR REPORT. Scientific and technical findings by NASA-sponsored contractors and grantees.

- CONFERENCE PUBLICATION. Collected papers from scientific and technical conferences, symposia, seminars, or other meetings sponsored or co-sponsored by NASA.

- SPECIAL PUBLICATION. Scientific, technical, or historical information from NASA programs, projects, and missions, often concerned with subjects having substantial public interest.

- TECHNICAL TRANSLATION. English-language translations of foreign scientific and technical material pertinent to NASA's mission.

Specialized services also include creating custom thesauri, building customized databases, and organizing and publishing research results.

For more information about the NASA STI program, see the following:

- Access the NASA STI program home page at *http://www.sti.nasa.gov*

- E-mail your question via the Internet to help@sti.nasa.gov

- Fax your question to the NASA STI Help Desk at 443-757-5803

- Phone the NASA STI Help Desk at 443-757-5802

- Write to:
  NASA STI Help Desk
  NASA Center for AeroSpace Information
  7115 Standard Drive
  Hanover, MD 21076-1320

NASA/TM–2010-216201

# Evaluation of a Small-Crack Monitoring System

*John A. Newman*
*Langley Research Center, Hampton, Virginia*

*William M. Johnston*
*Lockheed Martin Mission Services*
*Langley Research Center, Hampton, Virginia*

National Aeronautics and
Space Administration

Langley Research Center
Hampton, Virginia 23681-2199

February 2010

Available from:

NASA Center for AeroSpace Information
7115 Standard Drive
Hanover, MD 21076-1320
443-757-5802

# Abstract

*A new system has been developed to obtain fatigue crack growth rate data from a series of images aquired during fatigue testing of specimens containing small surface cracks that initiate at highly-polished notches. The primary benefit associated with replica-based crack growth rate data methods is preserving a record of the crack configuration during the life of the specimen. Additionally, this system has the benefits of both reducing time and labor, and not requiring introduction of surface replica media into the crack. Fatigue crack growth rate data obtained using this new system are found to be in good agreement with similar results obtained from surface replicas.*


# Introduction

Damage tolerance fatigue life predictions rely on experimentally-measured relations between the crack-tip driving force (ΔK) and the fatigue crack growth rate (d*a*/dN). The accuracy of these life predictions relies on the validity of experimental test data and the concept of crack-tip similitude, which presumes that crack growth rates are strictly a function of ΔK. However, it is well known that small fatigue cracks propagate at higher d*a*/dN (in comparison to long cracks at the same ΔK) and can propagate at ΔK values below the fatigue crack growth threshold observed for long cracks (refs. 1-5). These observations suggest that damage tolerance life predictions should be based on crack growth data appropriate for the anticipated crack lengths seen in service. Currently, automated standardized methods exist to generate long-crack data in a variety of specimen configurations (refs. 6-9), but no automated test methods exist for small surface cracks. Typically, fatigue crack growth rate data for small cracks are obtained using a series of surface replicas (refs. 3, 5). The primary drawback of using surface replicas to obtain crack growth rate data is that the method is both time and labor intensive.

In response to the need for an automated method to generate small fatigue crack growth rate data, a small crack monitoring system has been developed. This automated system captures high-resolution digital images of the crack starter notch region at regular intervals during fatigue tests. After the fatigue test is terminated, the digital images are analyzed to determine crack-length-versus-cycle-count data. From these data sets, d*a*/dN-versus-ΔK data are calculated. The objective of this report is to present test data obtained using the small crack monitoring system and to validate this automated system by comparing those results with data obtained using a well-established surface replica method.

# Description of the Small-Crack Monitoring System

The small crack monitoring system (SCMS) tracks the growth of small cracks in fatigue specimens using the concept of fringe deflectometry. Here, a series of white-light sinusoidal fringes, at $90^{o}$ offsets are projected onto a highly-polished specimen surface. A camera captures the images of the fringe pattern that is reflected off of the specimen surface, as shown schematically in Figure 1. Any changes in the curvature of the specimen surface will result in a distortion of the reflected fringe pattern. The highly localized stress state at the tip of a loaded crack and the residual deformation after crack growth result in a deformation field that can be seen as changes in the surface curvature. This system processes the fringe patterns into a picture representing the curvature of the surface as different grey levels. The cracks are visible in the curvature images, allowing crack lengths to be determined from the processed images.

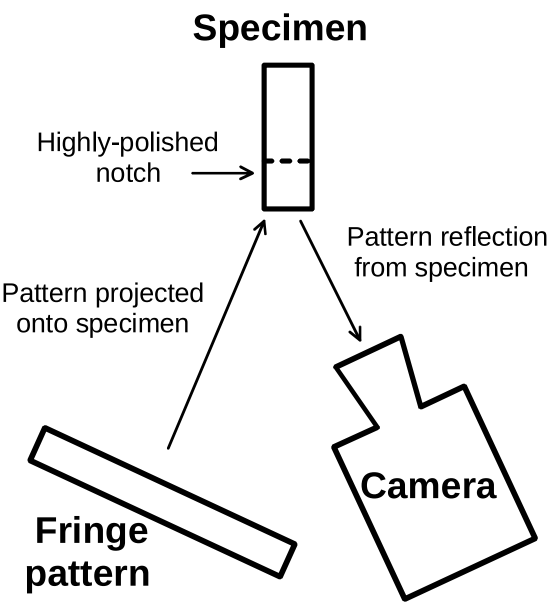


Figure 1. Schematic of Small-crack monitoring system.

A typical image captured by the SCMS is shown in Figure 2a. Here, the entire notch root region (see schematic; right side of Figure 2a) of an edge notch specimen is shown (specimen thickness = 5.1 mm). The notch surface has been polished to a near-mirror finish and the alternating white and black horizontal lines are the fringe pattern reflected off of the specimen. A distortion in the fringe pattern (local change in the thickness of the fringe pattern lines) is indicated in Figure 2a. Once analyzed by the SCMS, these digital images of the fringe patterns are used to create a curvature map. Essentially, the analysis determines the surface curvature that must be present to create the distortion observed in the fringe pattern. The curvature map corresponding to the image in Figure 2a is shown as Figure 2b. The shape of the surface curvature in the region of distortion indicated in Figure 2a appears to be typical of a crack. For the applied loads (for the orientation of Figure 2b, specimen is loaded in the vertical direction), a crack would be expected to propagate horizontally. A higher-magnification image of the curvature map surface crack region is shown as Figure 2c. Here, the curvature image appears to have a central horizontal line character, typical of surface cracks. The locations of the crack tips (ends of the central horizontal line section) are indicated in Figure 2c. The regions of curvature beyond the crack tips (highlighted with dashed circles) are the result of crack-tip deformations. The appearance of shear bands, lines of intense deformation emanating from the crack tip at near-45$^o$ angles, is typical of crack-tip deformation (refs. 10-13). Based on distortions in the horizontal fringe patterns, the raw images are converted into surface curvature maps and, analyzed to determine crack length at a specified cycle count. These data sets are then, ultimately, converted into crack-length-versus-cycle-count data.

## Test Plan for System Validation

Specimens used in this study were untested specimens from a previous small crack study (ref. 5) made from AISA 4340 steel plates, 9.5 mm thick supplied in the annealed condition. Specimens were machined such that the loading axis coincided with the rolling direction of the plate and were ground to a thickness of 5.1 mm. See Figure 3 for a schematic of the specimen configuration. Specimens were heat treated to a hardness of 45 HRC, by way of a one-hour soak at 840$^o$C, vacuum tempering at 440$^o$C for two hours, followed by furnace cooling in nitrogen gas. Average tensile properties of this material for

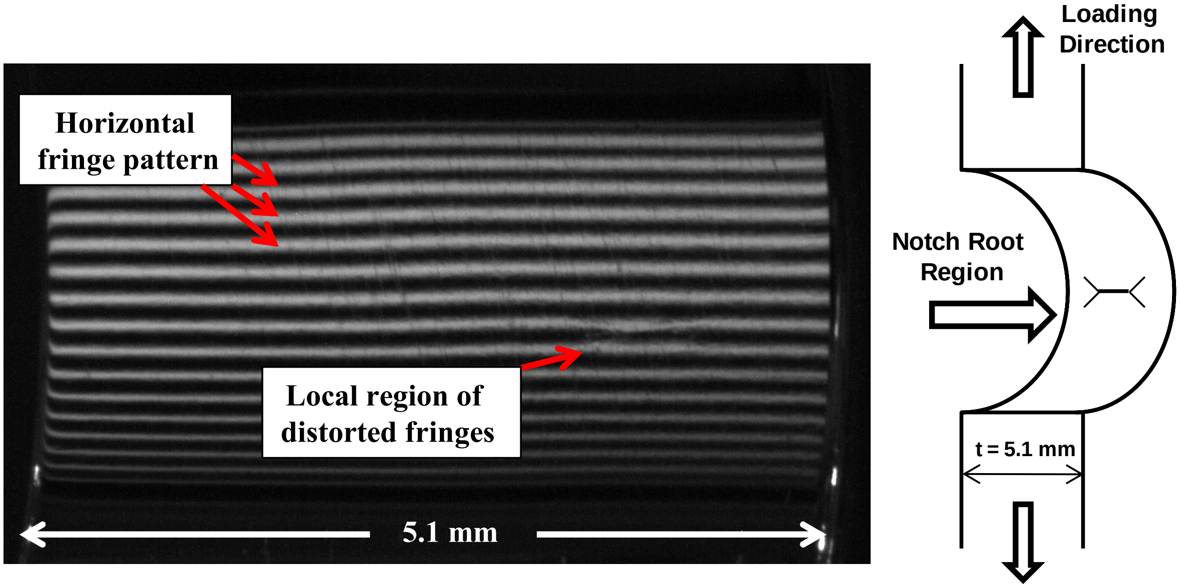


(a) Typical digital image of notch root region captured using small-crack monitoring system.

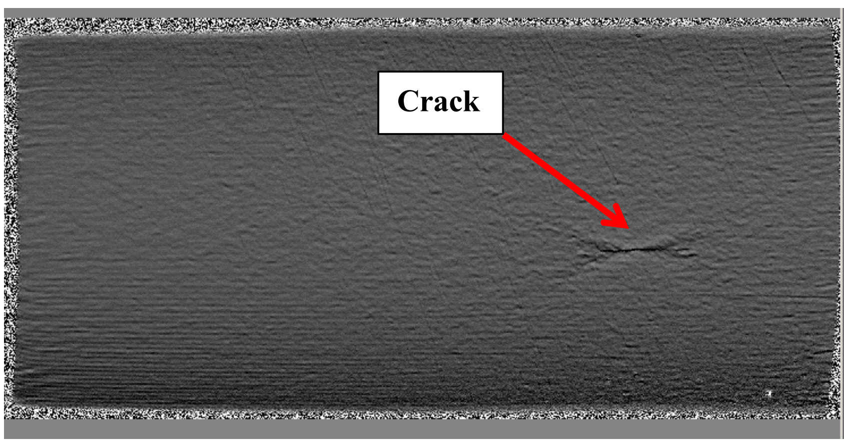


(b) Curvature map showing regions of local deformations near a fatigue crack.

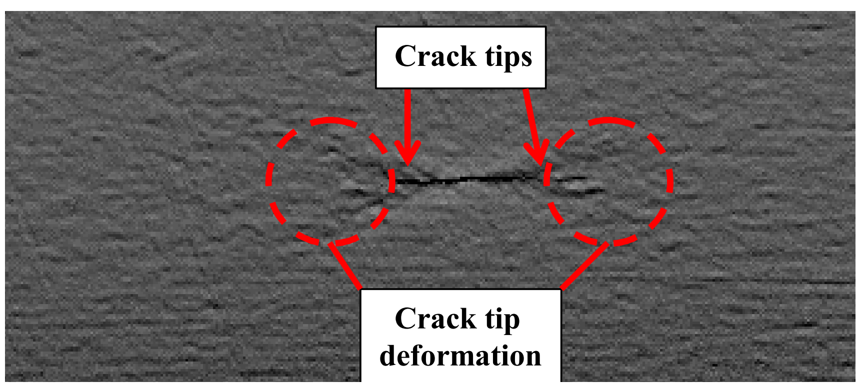


(c) Higher-magnification curvature map image of surface crack.

Figure 2. Typical image obtained from small-crack monitoring system.

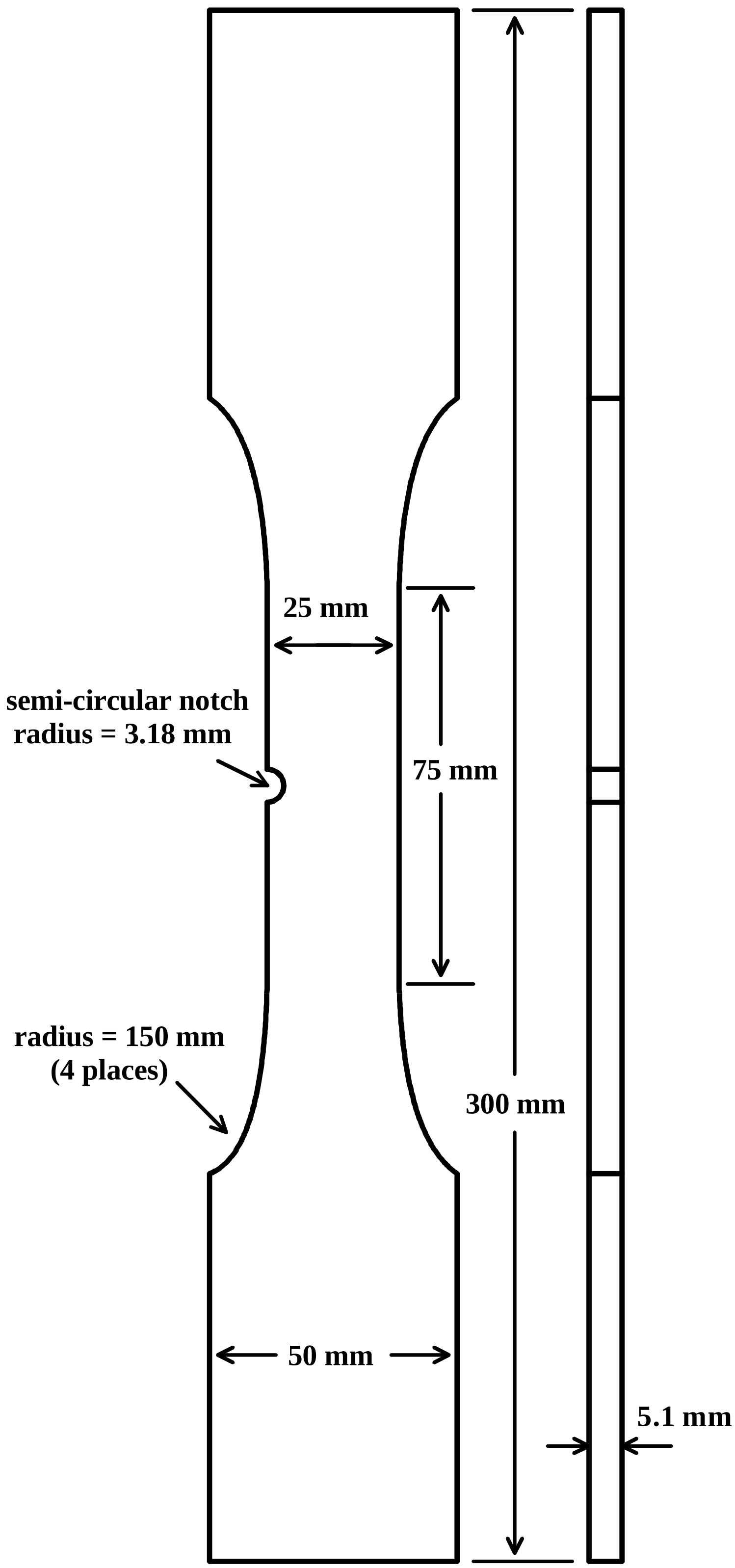


Figure 3. Specimen configuration.

ultimate stress, yield stress (0.2% offset), and elastic modulus were 1505 MPa, 1413 MPa, and 190 GPa, respectively. A description of the final microstructure, chemical composition, and results of individual tensile tests can be found in reference 5.

The notch (3.18 mm radius) in the specimen side has a stress concentration factor of 3.30, as calculated by the Boundary Force Method (ref. 14), and provided a compact high-stress region for crack initiation. The notch radius was achieved by final milling cuts of 0.25 mm, 0.13 mm, and 0.05 mm to minimize machining-induced residual stresses. Prior to testing, the specimen notch was polished to a near-mirror finish (approximately 8 RMS, meaning a surface roughness of 8 microns using the Root Mean Square method) to enhance crack detection.

## Experimental Results

Fatigue tests were conducted on AISA 4340 steel specimens (Figure 3) under constant amplitude loading, at a load ratio (ratio of minimum to maximum load) of R = 0 and a cyclic load frequency of 1 Hz. Testing was interrupted every 500 cycles by the automated test system to acquire digital images of the crack starter notch root region, where crack initiation is expected to occur. This sequence of 500 load cycles followed by image acquisition was repeated automatically until specimen failure occurred. Following specimen failure, the series of images acquired during testing were analyzed to determine distortions in the horizontal fringe patterns. These relative distortions between the series of four fringe images were used to determine curvature maps and, eventually, crack-length-versus-cycle-count data. From these results, the fatigue crack growth data were calculated.

The fatigue crack growth rate, d*a*/dN, was calculated using the secant method and the incremental polynomial method described in ASTM E647. Using the secant method, fatigue crack growth rate was calculated as,

$$\mathrm{d}a/\mathrm{dN} = \frac{a_{\mathrm{i+1}} - a_{\mathrm{i}}}{\mathrm{N}_{\mathrm{i+1}} - \mathrm{N}_{\mathrm{i}}} \tag{1}$$

where $a_i$ is a crack length corresponding to cycle count $N_i$, and $a_{i+1}$ and $N_{i+1}$ are crack length and cycle count values corresponding to the next available data. The crack length used to calculate ΔK, from this two point linear fit method, is taken as the midpoint (average *a*) of the crack growth increment. Using the incremental polynomial method helps reduce error induced by noisy experimental data by averaging over more data points. In comparison, the Secant Method (equation 1) uses only two data points. The incremental polynomial method fits a parabola to successive sets of seven points of data. The fatigue growth rate is calculated as the derivative of this fit evaluated at the center point. The crack length used to calculate ΔK is taken from the center of the fit. Refer to reference 6 for additional information on the incremental polynomial method.

The corresponding value of ΔK is calculated with assumptions that (1) the crack is a semi-circular surface crack, (2) the crack does not interact with other cracks, and (3) the crack length is small relative to the specimen dimensions of thickness, width, and notch radius. Values of ΔK are computed as,

$$\Delta \mathrm{K} = 0.73 \cdot \mathrm{k_t} \cdot \frac{\Delta \mathrm{P}}{\mathrm{A}} \cdot \sqrt{\pi a} \tag{2}$$

where $k_t$ is the stress concentration factor associated with the notch (equal to 3.30 for the specimens used), ΔP is the cyclic applied load, A is the cross sectional area of the specimen at the notch, and the factor of 0.73 corresponds to the geometry correction factor associated with a surface crack (ref. 15).

Crack length data from two tests are plotted in Figure 4 and 5 (open symbols) along with data obtained from a previous study (ref. 5) using surface replicas (closed symbols). The crack growth results reduced with the secant method are plotted in Figure 4 and similar data obtained using the incremental polynomial method are plotted in Figure 5. The maximum loads used during the first test (SCMS test #1) and second test (SCMS test #2) were 46.7 kN (10.5 kips) and 40.0 kN (9.0 kips), respectively. The second test was performed at a lower load in an effort to generate crack growth data at lower ΔK values to match the near-threshold performance of the surface replica method. Based on the fatigue crack growth rate data of Figure 4, the results obtained using the small-crack monitoring system are in good agreement with data obtained using surface replicas. The variability or "scatter" in the fatigue crack growth rate data is typical of small cracks (refs. 1-5). Typically, at low ΔK, where crack sizes are smaller, microstructural features are thought to be significant contributors to this scatter. The surface crack length for three data points of the first SCMS test are shown in the figure. Here, the SCMS tracked the crack from an initial crack length of approximately 50 μm (corresponding to ΔK = 7.8 MPa√m) until the crack grew to failure. The results of Figure 5 show similar agreement with the replica-based data of reference 5 (AGARD), although these sets of data appear to diverge at low values of ΔK (ΔK < 8 MPa√m).

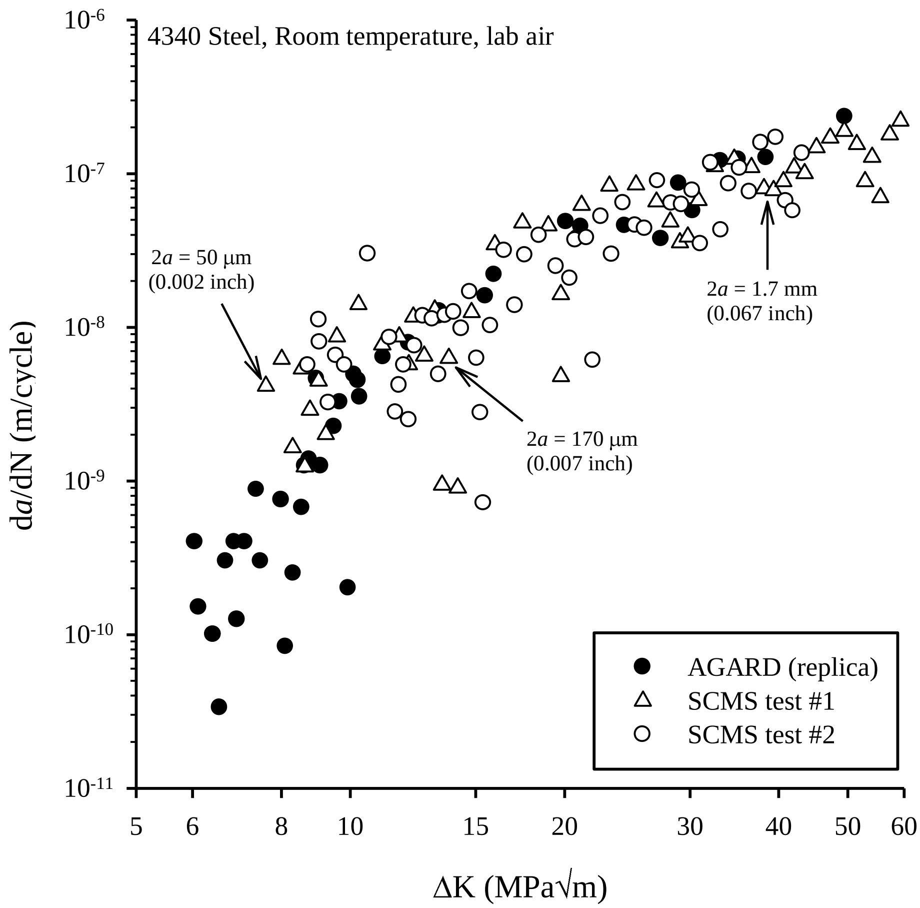


Figure 4. Crack growth data for small surface cracks in 4340 steel using the secant method.

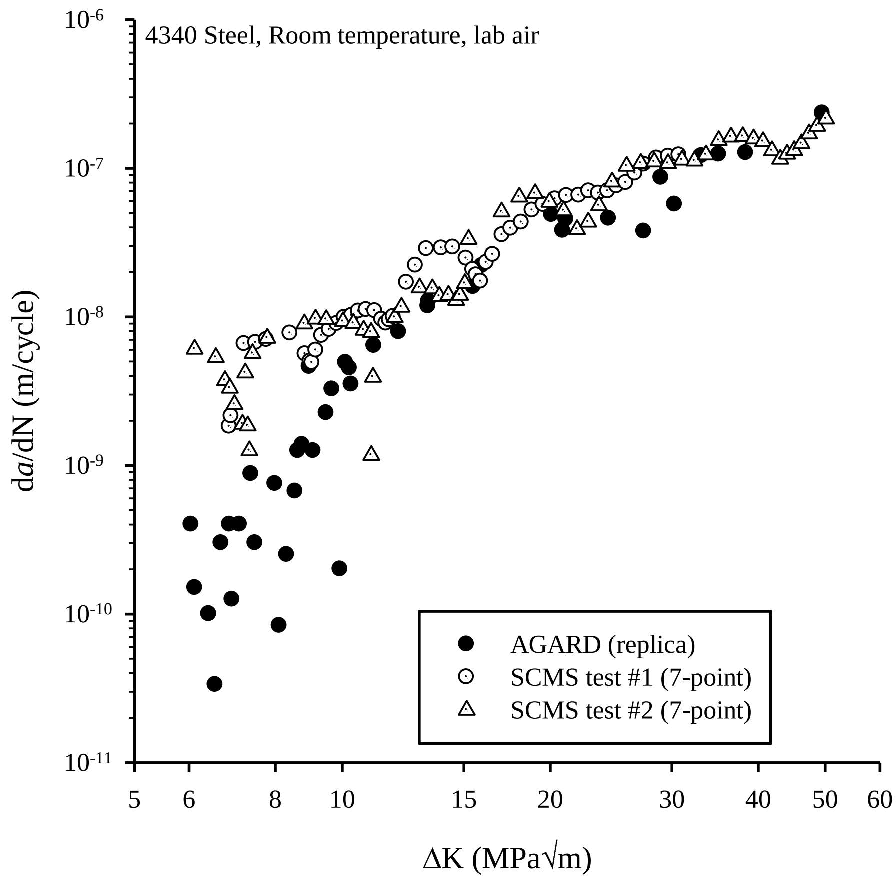


Figure 5. Crack growth data for small surface cracks in 4340 steel the incremental polynomial method.

## Discussion of Results

The experimental results shown in Figure 4 indicate that the SCMS produces the same crack growth rate data as the surface-replica method of reference 5, at least for $\Delta K > 8$ MPa√m. Fatigue tests were attempted at loads below $P_{max} = 40.0$ kN (9.0 kips), but these loads did not result in fatigue cracking before testing was terminated. Based on the results presented in this paper, the SCMS produces the same fatigue crack growth data (Figure 4 and 5) as a well-established surface replica method, but has the significant advantage of being automated reducing both the labor and time associated with generating small-crack data. Additional study is needed to conclusively demonstrate that the system can deliver results consistent with replica-based methods for a wide range of loading and alloys.

The impact of an automated small-crack system on damage tolerance life management is significant. Although many (perhaps even a majority of) service failures are the result of initiation and propagation of small cracks, the majority of available crack growth data in the literature are generated using long-crack specimens. One reason for the relative scarcity of small-crack data is the labor burden associated with small-crack testing. Automated systems like the one described in this paper would make obtaining small-crack data easier to obtain and, eventually, should increase the available small-crack data for analysis.

## Summary

Experimental fatigue crack growth results, obtained using a newly-developed automated small-crack monitoring system, are presented here and compared with results obtained using surface replicas, a trusted and well-established method of obtaining small-crack growth data. The results presented showed both methods to be in good agreement, suggesting that the automated small-crack system is capable of reproducing small-crack results of a well-established method known to produce reliable results.

## References

1. S. Pearson, "Initiation of Fatigue Cracks in Commercial Aluminum Alloys and the Subsequent Propagation of Very Small Cracks," *Engineering Fracture Mechanics*, Vol. 7, 1975, pp. 235-247.

2. H. Kitagawa and S. Takahashi, "Applicability of Fracture Mechanics to Very Small Cracks or the Cracks in the Early Stage," *Proceedings of the 2nd International Conference on Mechanical Behavior of Materials*, Boston, Massachusetts, 1976, pp. 627-631.

3. R.O. Ritchie and J. Lankford, Eds., *Small Fatigue Cracks, Proceedings of the 2nd Engineering Foundation International Conference*, Santa Barbara, California, January 5-10, 1986.

4. K.S. Ravichandran, R.O. Ritchie, and Y. Murakami, Eds., *Small Fatigue Cracks: Mechanics, Mechanisms and Applications, Proceedings of the 3rd Engineering Foundation International Conference*, Oahu, Hawaii, 1998.

5. M.H. Swain, R.A. Everett, Jr., J.C. Newman, Jr., and E.P. Phillips, "The Growth of Short Cracks in 4340 Steel and Aluminum-Lithium 2090," AGARD Report No. 767, Short-Crack Growth Behaviour in Various Aircraft Materials, August 1990, Advisory Group for Aerospace Research and Development.

6. Annual Book of ASTM Standards, Vol. 3.01, "Standard Test Method for Measurement of Fatigue Crack Growth Rates," American Society for Testing and Materials (ASTM), West Conshohocken, PA, 2007.

7. J.K. Donald and D.W. Schmidt, "Computer-Controlled Stress Intensity Gradient Technique for High Rate Fatigue Crack Growth Rate Testing," *Journal of Testing and Evaluation*, JTEVA, Vol. 8, 1980, pp. 19-24.

8. A. Saxena, S.J. Hudak, Jr., J.K. Donald, and D.W. Schmidt, "Computer-Controlled Decreasing Stress Intensity Technique for Low Rate Fatigue Crack Growth Testing," *Journal of Testing and Evaluation*, Vol. 6, 1978, pp. 167-174.

9. W.F. Deans and C.E. Richards, "A Simple and Sensitive Method of Monitoring Crack and Load in Compact Fracture Mechanics Specimens Using Strain Gages," *Journal of Testing and Evaluation*, Vol. 7, 1979, pp. 147-154.

10. J.W. Hutchinson, "Plastic Stress and Strain Fields at a Crack Tip," *Journal of the Mechanics and Physics of Solids*, Vol. 16, 1968, pp. 337-347.

11. H. Tada, P.C. Paris, and G.R. Irwin, *Stress Analysis of Cracks Handbook*, Del Research Corporation, Hellertown, PA, 1985.

12. G.C. Sih, *Handbook of Stress Intensity Factors*, Lehigh University, Bethlehem, PA, 1973.

13. H. Gao, N. Alagok, M.W. Brown, and K.J. Miller, "Growth of Fatigue Cracks Under Combined Mode I and II Loads," ASTM STP 853, American Society for Testing and Materials, Philadelphia, PA, 1985, pp. 184-202.

14. P.W. Tan, I.S. Raju, and J.C. Newman, Jr., "Stress Intensity Factor Calculations Using the Boundary Force Method," NASA/TM-89158, 1987.

15. N.E. Dowling, *Mechanical Behavior of Materials*, 2nd Ed., Prentice Hall, Upper Saddle River, NJ, 1999, p. 302.

# REPORT DOCUMENTATION PAGE

*Form Approved*
*OMB No. 0704-0188*



**1. REPORT DATE** *(DD-MM-YYYY)*
01- 02 - 2010

**2. REPORT TYPE**
Technical Memorandum

**3. DATES COVERED** *(From - To)*

**4. TITLE AND SUBTITLE**
Evaluation of a Small-Crack Monitoring System

**5a. CONTRACT NUMBER**

**5b. GRANT NUMBER**

**5c. PROGRAM ELEMENT NUMBER**

**6. AUTHOR(S)**
Newman, John A.; Johnston, William M.

**5d. PROJECT NUMBER**

**5e. TASK NUMBER**

**5f. WORK UNIT NUMBER**
329231.01.07.04.50

**7. PERFORMING ORGANIZATION NAME(S) AND ADDRESS(ES)**
NASA Langley Research Center
Hampton, VA 23681-2199

**8. PERFORMING ORGANIZATION REPORT NUMBER**
L-19832

**9. SPONSORING/MONITORING AGENCY NAME(S) AND ADDRESS(ES)**
National Aeronautics and Space Administration
Washington, DC 20546-0001

**10. SPONSOR/MONITOR'S ACRONYM(S)**
NASA

**11. SPONSOR/MONITOR'S REPORT NUMBER(S)**
NASA/TM-2010-216201

**12. DISTRIBUTION/AVAILABILITY STATEMENT**
Unclassified - Unlimited
Subject Category 26
Availability: NASA CASI (443) 757-5802

**13. SUPPLEMENTARY NOTES**

**14. ABSTRACT**
A new system has been developed to obtain fatigue crack growth rate data from a series of images aquired during fatigue testing of specimens containing small surface cracks that initiate at highly-polished notches. The primary benefit associated with replica-based crack growth rate data methods is preserving a record of the crack configuration during the life of the specimen. Additionally, this system has the benefits of both reducing time and labor, and not requiring introduction of surface replica media into the crack. Fatigue crack growth rate data obtained using this new system are found to be in good agreement with similar results obtained from surface replicas.

**15. SUBJECT TERMS**
Crack length; Digital images; Fatigue crack growth; Small crack

| 16. SECURITY CLASSIFICATION OF: a. REPORT | b. ABSTRACT | c. THIS PAGE | 17. LIMITATION OF ABSTRACT | 18. NUMBER OF PAGES | 19a. NAME OF RESPONSIBLE PERSON / 19b. TELEPHONE NUMBER *(Include area code)* |
|---|---|---|---|---|---|
| U | U | U | UU | 13 | STI Help Desk (email: help@sti.nasa.gov) / (443) 757-5802 |

**Standard Form 298** (Rev. 8-98)
Prescribed by ANSI Std. Z39.18